Dendrites Nanostructures of Co3O4 for the Selective Determination of Uric Acid

Ramesh Lal
Shah Abdul Latif University
Bhajan Lal Bhattia
Shah Abdul Latif University
Ali M. Alsalme
King Saud University
Asma A. Al-Othman
King Saud University
Ayman Nafady
King Saud University
Zafar Hussain Ibupoto (zaffar.ibhupoto@usindh.edu.pkk)
University of Sindh https://orcid.org/0000-0002-6756-9862

Research Article

Keywords: Hydroxide functionalized MWCNTs, cobalt oxide, dendrite nanostructures uric acid, phosphate buffer solution, enzyme free sensor

Posted Date: March 17th, 2021

DOI: https://doi.org/10.21203/rs.3.rs-296806/v1

Version of Record: A version of this preprint was published at Journal of Materials Science: Materials in Electronics on July 15th, 2021. See the published version at https://doi.org/10.1007/s10854-021-06325-3.

Abstract

The gout is mainly found due to accumulation of uric acid crystals into the joints which produces the inflammatory symptoms. Thus, it is highly demanded to detect uric acid from our body. Herein, we used wet chemical method for the preparation of composite material of cobalt oxide (Co_3O_4) with hydroxide functionalized multi-walled carbon nanotubes (MWCNTs). The analytical techniques such as scanning electron microscopy (SEM), powder X-ray diffraction (XRD), energy dispersive spectroscopy (EDS) and Infra-red spectroscopy (FTIR) were used to characterize the composite material. The Co_3O_4 exhibits a dendrite morphology and very well chemically coupled with MWCNTs. The elemental analysis confirmed the presence of Co, O and C as main constituent of the composite material. The Co_3O_4 exhibits a cubic unit cell crystallography in the composite system. The FTIR study has revealed the characteristic bands of Co-O bands in the composite material. The cyclic voltammetry was used to study the electrochemical properties of prepared materials. The composite sample with highest percentage of MWCNTs showed an excellent electrochemical activity towards the oxidation of uric acid in phosphate buffer solution pH 7.3. The enzyme free uric acid sensor possessed a linear range of 0.1 mM to 3 mM with a quantified limit of detection of 0.005 mM. The modified electrode is stable, selective, and very sensitive towards uric acid, therefore it may be used for the monitoring of uric acid from clinical samples. The proposed composite material is low cost, and earth abundant, thus it can be of great interest for energy and biomedical fields.

1. Introduction

The human fluids such as urine and blood contain uric acid (UA). The uric acid is bioorganic compoundin nature and produced in our body as a byproduct during the metabolism. It is also heavily present in some of the food products. The presence of uric acid is highly notorious and harmful for the human body as our body does not have enzyme to decompose uric acid into non-toxic products. The large deposition of uric acid in our body may give birth to disease like gout or storage of stones in kidney. The gout is mainly found due to accumulation of uric acid crystals into the joints which produces the inflammatory symptoms [1]. Thus, it is highly demanded to detect uric acid from our body which could be associated to the other diseases like metabolic syndrome, anxiety/hypertension, kidney failures and cardiovascular [2, 3]. The standard methods used for the determination of uric acid are enzymatic techniques [4], reduction of phosphotungstic acid [5], and chromatography/mass spectrometry [6, 7]. The phosphotungstic reduction approach has superiority over other methods because of easiness in operation. However, it is limited by the interference effect. But the enzyme-based methods are very specific but not suitable due to high cost of enzyme, complicated enzyme immobilization process and sensitive to environmental conditions, therefore they cannot be used at large scale. The chromatography/ mass spectrometry is a good choice due to high sensitivity and reliability, but the used instruments are very costly. The electrochemical methodology is recently evolved which applies the cyclic voltammetry [8], pulse voltammetry [9] and chronoamperometry [10, 11]. The use of nanostructured materials for the modification of working electrode is of great interest to produce simple, low cost, stable and selective analytical devices for the detection of uric acid. For this purpose, metal oxides of 3-d series are of great

interest and they have excited the researchers in the fields of electrochemical sensing [12], supercapacitors [13], and energy conversion and storage applications [14] because of their good catalytic properties, fast electron communication, and excellent compatibility with biomaterials [15]. Among the metal oxides, cobalt oxide (Co_3O_4) is largely investigated and produced into variety of morphologies such as nanowires, nanoparticles, and nano spindles [16, 17]. The attractive properties of Co_3O_4 are significant stability in basic electrolyte, mixed valence states and narrow optical band gap [18]. However, pristine nanostructured Co_3O_4has tendency to agglomerate and poor electrical conductivity consequently weak electrochemical activity.

On other hand, the carbon nanotubes are used as supportive stuff during the development of sensor devices because of their attractive, and unique mechanical, physical, and electrical properties [19, 20, 2, 22, 23]. The superfast conductivity, internal structure and mechanical stability enables them to act as efficient substrate. The carbon nanotubes exhibit high electrical conductivity of 104 S cm^{-1}, specific surface area of 200–900 m^2 g^{-1}, and show a large porosity for the deposition of other nanostructured materials and highly improve their dispersion in a solvent [24–37]. The hypothesis of the present study is to produce a composite of Co_3O_4 with multi-walled carbon nanotubes in such a way that agglomeration of Co_3O_4 is minimized and further its conductivity should be increased. We functionalized the MWCNTs with highly alkaline solution of sodium hydroxide enabling them with rich hydroxide surface which further could act as nucleates for the bonding of cobalt ions, consequently well-controlled morphology of Co_3O_4 is obtained. Thus, we exploited the high electrical conductivity and specific surface area of MWCNTs and chemically anchored dendrites nanostructures of Co_3O_4. Importantly, there is no report on the Co_3O_4/MWCNTs composite material used for the non-enzymatic sensing of uric acid.

In this study, we report a facile non-enzymatic analytical electrode consisting Co_3O_4/MWCNTs composite for the sensing of uric acid in PBS of pH 7.3. The composite material was prepared via wet chemical method and physically studied with different analytical SEM, EDS, XRD and FTIR. The non-enzymatic sensor is selective and stable and shows a linear range of 0.1 mM to 3 mM. The material characterization and sensor performance show that the composite material could be applied in other medical and energy related fields.

2. Materials And Methods

2.1. Chemicals

The analytical grade cobalt nitrate hexahydrate Co $(NO_3)_2.6H_2O$, urea (CH_4N_2O), 99.5% ethanol, MWCNT, were received from Sigma-Aldrich Karachi (Pakistan). The washing of glassware was done with 3 M HNO_3 and deionized water. They were dried at 95 ^oC. An aqueous chemical growth was used for the synthesis of various Co_3O_4-MWCNTs composites. The MWCNTs were rinsed with 2M sulphuric acid and washed several times with deionized water. Then bare MWCNTs were functionalized with 3M NaOH for 30 minutes. The purpose of hydroxide functionalization was to accelerate the growth kinetics of Co_3O_4

and to control on the morphology. Then different amounts of hydroxide functionalized MWCNTs such as 25, 50, 75 mg were taken in three beakers and weighed amount of 2.92 g of cobalt nitrate hexahydrate and 0.6 g of urea was added in each beaker. The volume of each beaker was made up to 100 mL with deionized water. Each beaker was labelled as sample 1, sample 2 and sample 3. Then the beakers were kept at 95 ^{o}C for 6 h in electric oven. After the hydrothermal treatment and cooling of beakers, the grown product was collected on ordinary filer paper and washed with deionized water. Then material was dried and kept in muffle furnace at 500 ^{o}C for 5 h in air for the complete conversion of hydroxide phase into oxide. Finally, a black product of $Co_3O_4$was obtained and used for physical and electrochemical investigations. A pristine sample of Co_3O_4 was also prepared by the same process without the addition of MWCNTs. The structure and composition of each sample was investigated with XRD, SEM and EDS. The SEM was done at 15 kV and experimental conditions for XRD were CuKα radiation (λ = 1.54050 Å), 45 mA, 45 kV and (2θ) scale range from 10 to 85°. The electrochemical characterization of prepared samples was done with electrochemical workstation CHI 760D from USA and associated with software CHI 9.22. The electrochemistry was studied with three electrode cell setup, where silver-silver chloride as reference electrode, platinum wire as counter electrode and modified glassy carbon electrode (GCE) as working electrode. The uric acid determination was performed in 0.1M PBS of pH 7.3. The GCE with a diameter of 3 mm was pasted with alumina powder of size 1 μm and 0.05μm. Then it was rubbed with silica paper and cleaned by deionized water. For a better cleaning, GCE was kept in ethanol in ultrasonic bath for 20 mints. Each material with an amount of 5 mg was suspended in 1 mL of ethanol and 50 μL of 5% Nafion and coated on the GCE using drop casting technique. Then modified GCE was dried naturally and ready for electrochemical studies. The 5 mM uric acid solution was prepared in 0.1M PBS of pH 7.3. Then fresh solutions of uric acid with low concentrations were also prepared in phosphate buffer solution using dilution formula

3. Results And Discussion

3.1. Structural and compositional analysis of prepared Co_3O_4 nanostructures

The prepared materials were studied structurally through scanning electron microscope as enclosed in Fig. 1. The pristine sample of Co_3O_4 carries a dendrite like morphology as shown in Fig. 1a. The deposition of same dendrite Co_3O_4 nanostructure on hydroxide functionalized MWCNTs were obtained as shown in Fig. 1b-d. The use of different quantities of MWCNTs did not greatly effect on the morphology of Co_3O_4, but they have minimized the space between each dendrite structure and giving out a compact dendrite morphology of Co_3O_4. The hydroxide functionalized MWCNTs facilitated the significant electrical communication among the dendrite nanostructures of Co_3O_4, therefore an improved electrical signal is achieved. The chemical composition of composite samples was studied by EDS and it confirmed the quantified amount of C, Co and O and no other impurity or product was identified Fig. 2. The EDS showed the successive amount of MWCNTs in the composite samples. The crystalline phase of pristine Co_3O_4

and its composites with MWCNTs is depicted in Fig. 3a. All the diffraction patterns are evolved from the cubic phase of Co_3O_4 and they are fully authenticated by reference card no = 96-900-5889. The growth orientation of all samples is favorable along the 113-crystal plane. The XRD study could not find any diffraction for the MWCNTs due to use to their very amount in the composite samples and only Co_3O_4 crystal features are detected. The presence of Co_3O_4 on MWCNTs was studied by FTIR study Fig. 3b. The spectra for the pristine Co_3O_4 and its composite samples with MWCNTs were measured. The bands related metal-oxygen connectivity was seen at 545 to 576 cm^{-1} [38, 39]. The band at 665 cm^{-1} is linked to Co^{3+} in the octahedral vicinity and the stretching band of Co^{2+} in the tetrahedral vicinity [40] and it provides a clear indication of single crystalline Co_3O_4 and well in agreement with XRD results. Furthermore, the shift in the composite samples revealed the strong interaction of Co_3O_4 with MWCNTs [41].

3.2. Electrochemical uric acid oxidation

Figure 4a shows the influence of different electrolytes on the electrochemical signal of the uric acid using modified GCE with sample 3 in 0.1mM uric acid and the electrolytes were Britton–Robinson buffer (BRB) buffer of pH 5, NaOH with pH 13 and Phosphate buffer solution of pH 7.3. It can be visualized that a prominent oxidation peak with enhanced peak current is revealed in the phosphate buffer solution Fig. 4a. The electrolyte study was carried to bring the analytical device performance close to the physiological conditions. However, the electrochemical signal of sensor in NaOH and BRB buffer is also good but less intense compared to the phosphate buffer solution. For the better understanding, the electrochemical signal of sample 3 modified GCE was also measured in the phosphate buffer solution without uric acid and with 0.1mM uric acid. From Fig. 4b, it is obvious that no oxidation peak was seen in the electrolyte, however a visible and well resolved oxidation peak for the sampl3 3 was observed in uric acid. To see the activity of sensor electrode for the various uric acid concentrations and the CV curves were measured Fig. 4c. The increase in the uric acid concentration brought linear enhancement in the oxidation peak current and it revealed a significant sensitivity towards uric acid. The linear range of analytical electrode for the uric acid was from 0.1mM to 3 mM. A calibration pilot was built by plotting oxidation peak current versus different concentrations of uric acid Fig. 4d. The linear fitting demonstrated robust analytical device features with a regression coefficient of 0.99. The quantified limit of detection of modified electrode was 0.005 mM. The prepared samples of Co_3O_4, and its composites with MWCNTs were further analyzed in 0.1mM uric acid and their performance is compared Fig. 5a. The most active composite was sample 3 which introduced an excellent oxidation peak current during the oxidation of uric acid, and it is more prominent than the other materials such as pristine Co_3O_4, sample 1 and sample 2.The interference study was also carried on sample 3 to monitor the sensing capability of sensor under the environment of competing species during the uric acid detection Fig. 5b. The interfering substances such as urea, lactic acid, ethanol, and mixture of them were used and their concentration was 0.1mM. An equal volume of these interfering species was used along with uric acid and it suggests that sensor did not show any electrochemical response to these substances, but a only a uric acid oxidation peak is demonstrated Fig. 5b. The electrode kinetics of sample 3 was also studied at different sweeping scans in

0.1mM uric acid Fig. 5c and there was seen a continuous increase in peak current with increasing scan rate which is another indication of diffusion controlled kinetics of the electrode. The scan rates were ranged from 10 mV/s-90 mV/s Fig. 5c. The stability is another factor for the sample 3 modified electrode it was investigated in 0.1mM uric acid solution Fig. 5d. The CV curves were recorded at 50 mV/s and there was no fluctuation of current and the potential and the electrode has ability to retain the oxidation features.

4. Conclusions

In summary, the Co_3O_4 composite with MWCNTs were fabricated via solution process and used for the sensing of uric acid in PBS of pH 7.3. The MWCNTs offered the high porosity, inter-particle interaction and conductivity for the Co_3O_4. The composite materials are well characterized by SEM, EDS, XRD and FTIR. The dendrite morphology of Co_3O_4 composites are evolved on the hydroxide functionalized MWCNTs and they contain cobalt, oxygen and carbon as the main atoms in the composition. The sample 3 of Co_3O_3 composite with highest percentage of MWCNTs modified GCE exhibits a good selectivity, stability, and well-defined oxidation peak for the uric acid. The sensor possesses a linear range from 0.1mM to 3 mM uric acid with quantified limit of detection 0.005 mM. The proposed composite material is, low cost, and has significant electrochemical activity which could be used for wide range of biomedical applications.

Declarations

Acknowledgement:

The authors extend their sincere appreciation to the Deanship of the Scientific Research at King Saud University for funding this project through Research Group (RG #236)

Competing interests:

All the Authors declare no competing interests in this study

References

1. K.L. Rock, H. Kataoka, J.J. Lai, Nat. Rev. Rheumatol. **9**(1), 13 (2013)
2. Z. Soltani, K. Rasheed, D.R. Kapusta, E. Reisin. *Current hypertension reports* **15**(3), 175–181 (2013)
3. M. Alderman, K.J.V. Aiyer, Curr. Med. Res. Opin. **20**(3), 369–379 (2004)
4. M. Jelikic-Stankov, P. Djurdjevic, D. Stankov. *Journal of the Serbian Chemical Society* **68**, 8–9 (2003) pp. 691–698.
5. V.J. Pileggi, J. Di Giorgio, D.K. Wybenga, Clin. Chim. Acta. **37**, 141–149 (1972)

6. X.H. Dai, X. Fang, C.M. Zhang, R.F. Xu, B. Xu. *Journal of Chromatography B* **857**(2), 287–295 (2007)
7. X.Y. Liu, Y. Luo, C.Y. Zhou, A. Peng, J.Y. Liu. *Bioanalysis* **9**(22), 1751–1760 (2017)
8. K.Y. Zhang, N. Zhang, L. Zhang, H.Y. Wang, H.W. Shi, RSC Adv. **8**, 5280–5285 (2018) no. 10)
9. D. Thirumalai, D. Subramani, J.H. Yoon, J. Lee, H.J. Paik, S.C. Chang, New J. Chem. **42**(4), 2432–2438 (2018)
10. K. Movlaee, P. Norouzi, H. Beitollahi, M. Rezapour, B. Larijani, Int. J. Electrochem. Sci. **12**, 3241–3251 (2017)
11. Y. Bu, W.L. Dai, N. Li, X.R. Zhao, X. Zuo. *Journal of energy chemistry* **22**, 685–689 (2013)
12. C.D. Georgakopoulos, F.N. Lamari, I.N. Karathanasopoulou, V.S. Gartaganis, N.M. Pharmakakis, N.K. Karamanos, Biomed. Chromatogr. **24**(8), 852–857 (2010)
13. L.J. Han, R.J. Liu, C.S. Li, H.H. Li, C.X. Li, G.J. Zhang, J.N. Yao, Journal of Materials Chemistry 22,17079(2012)
14. Y.J. Hu, Q. Shao, P. Wu, H. Zhang, C.X. Ca, Electrochem. Commun. **18**, 96–99 (2012)
15. Y. Hu, P. Wu, Y. Yin, H. Zhang, C. Cai, Appl. Catal. B **111**, 208–217 (2012)
16. Q.T. Huang, S.R. Hu, H.Q. Zhang, J.H. Chen, Y.S. He, F.M. Li, W. Weng, J.C. Ni, X.X. Bao, Y. Lin. *Analyst* **138**(18), 5417–5423 (2013)
17. K.D. Kong, F. Yan, Z. Han, J. Xu, X. Guo, L. Chen, RSC Adv. **6**, 67481–67487 (2016)
18. Q.T. Huang,., H.Q. Zhang, S.R. Hu, F.M. Li, W. Weng, J.H. Chen, Q.X. Wang, Y.S. He, W.X. Zhang, X. X. Bao. *Biosensors and Bioelectronics* **52**, 277–280 (2014)
19. J. Zhang, G. Wang, Z. Liao, P. Zhang, F. Wang, X. Zhuang, E. Zschech, X. Feng, Nano Energy **40**, 27–33 (2017)
20. L.C. Seitz, C.F. Dickens, K. Nishio, Y. Hikita, J. Montoya, A. Doyle, C. Kirk, A. Vojvo dic, H.Y. .Hwang, J.K. Norskov, T. F. Jaramillo. *Science* **353**(6303), 1011–1014 (2016)
21. X. Liang, L. Shi, Y. Liu, H. Chen, R. Si, W. Yan, Q. Zhang, G.-D. Li, L. Yang, X. Zou, Angew. *Angewandte Chemie International Edition* **58**(23), 7631–7635 (2019)
22. M. Zhu, Q. Shao, Y. Qian, X. Huang. *Nano Energy* **56**, 330–337 (2019)
23. Y. Pi, J. Guo, Q. Shao, X. Huang. *Chemistry of Materials* **30**(23), 8571–8578 (2018)
24. Y. Pi, Q. Shao, P. Wang, J. Guo, X. Huang. *Advanced Functional Materials* **27**(27), 1700886 (2017)
25. S. Kumari, B.P. Ajayi, B. Kumar, J.B. Jasinski, M.K. Sunkara, J.M. Spurgeon, Energy Environ. Sci. **10**(11), 2432–2440 (2017)
26. H. K. Maleh, M. Moazampour, A. A. Ensafi, S. Mallakpour, M. Hatami. *Environmental Science and Pollution Research* 21 (9) (2014), pp. 5879–5888.
27. J.M. R.Shahmiri, V. Aarts, R. Bennani, M. Das, Swain, Int J Dent 13,(2013)
28. A. Pahlavan, H. Karimi-Maleh, F. Karimi, M.A. Amiri, Z. Khoshnama, M.R. Shahmiri, M. Keyvanfard, Materials Science and Engineering: C **45**, 210–215 (2014)
29. W. Wu,, H. Min, H. Wu,Y. Ding &S.Yang,Nature 23, (2016)

30. G. K.Paunovic, B. Belojevic, Jakovljevic. *Noise and health* **15**(65), 253 (2013)
31. K. Guo, Z. Zou, J. Du, Y. Zhao, B. Zhou, C. Xu, Chem. Commun. **54**(79), 11140–11143 (2018)
32. J.C. Fontecilla-Camps, A. Volbeda, C. Cavazza, Y. Nicolet. *Chemical reviews* **107**(10), 4273–4303 (2007)
33. J.W. Peters, W.N. Lanzilotta, B. J. Lemon. L. C. Seefeldt. Science **282**(5395), 1853–1858 (1998)
34. D. Kong, J.J. Cha, H. Wang, H.R. Lee, Y. Cui, Energy Environ. Sci. **6**(12), 3553–3558 (2013)
35. M.S. Faber, R. Dziedzic, M.A. Lukowsik, N.S. Kaiser, Q. Ding, S. Jin, J. Am. Chem. Soc. **136**(28), 10053–10061 (2014)
36. S. Peng, L. Li, X. Han, W. Sun, M. Srinivasan, S.G. Mhaisalkar, F. Cheng, Q. Yan, J. Chen, S. Ramakrishna, Angew. Chem. **126**(46), 12802–12807 (2014)
37. Z. Peng, D. Jia, A.M. Al-Enizi, A.A. Elzatahry, G. Zheng, Advanced Energy Materials **5**(9), 1402031 (2015)
38. T. Ozkaya, A. Baykal, M.S. Toprak, Y. Koseoğlu, Z. Durmuş, Open Chemistry **7**(3), 410–414 (2009)
39. R. Yuvakkumar, A.J. Nathanael, S. I. Hong. *RSC advances* **4**, 44495–44499 (2014) 84)
40. J. Xu, P. Gao, T. S. Zhao. *Energy & Environmental Science* **5**(1), 5333–5339 (2012)
41. P. Thangasamy, K. Selvakumar, M. Sathish, S. Murugesan, S. Kumar, R. Thangamuthu. *Catalysis Science & Technology* **7**(5), 1227–1234 (2017)

Figures

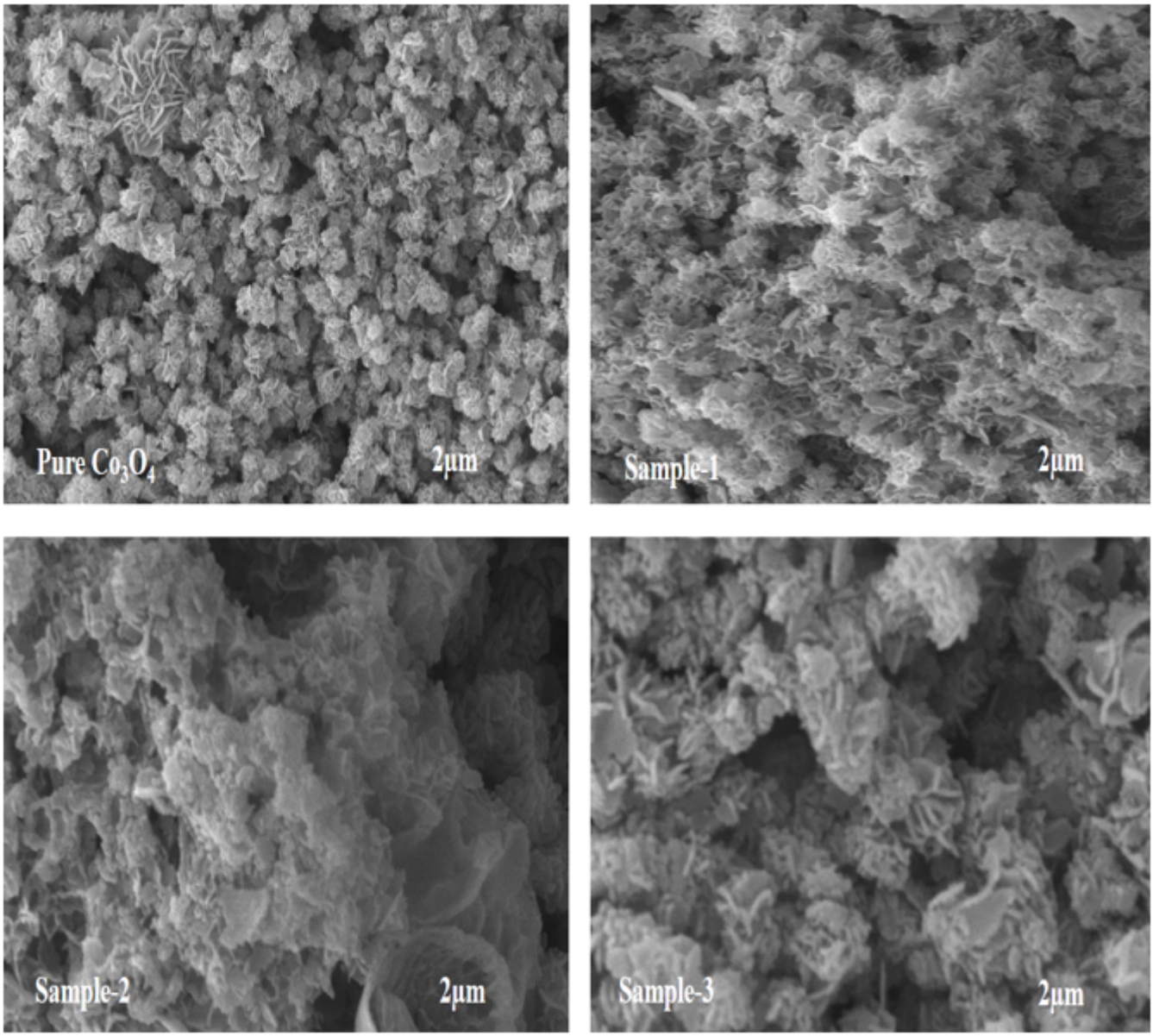

Figure 1

SEM images a. pure Co3O4, b. sample 1, c. sample 2, d. sample 3

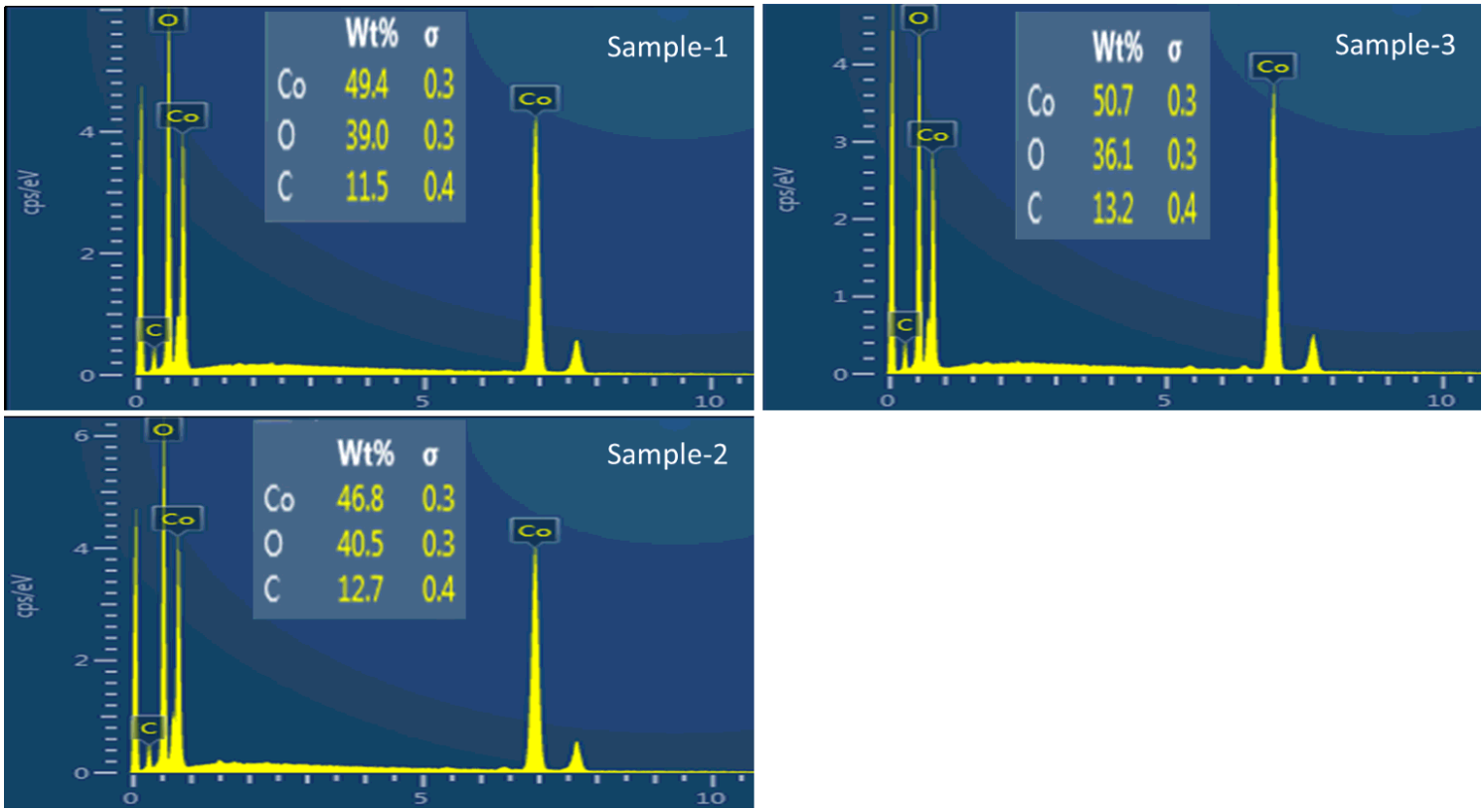

Figure 2

EDS spectra a. sample 1, b. sample 2, c. sample 3

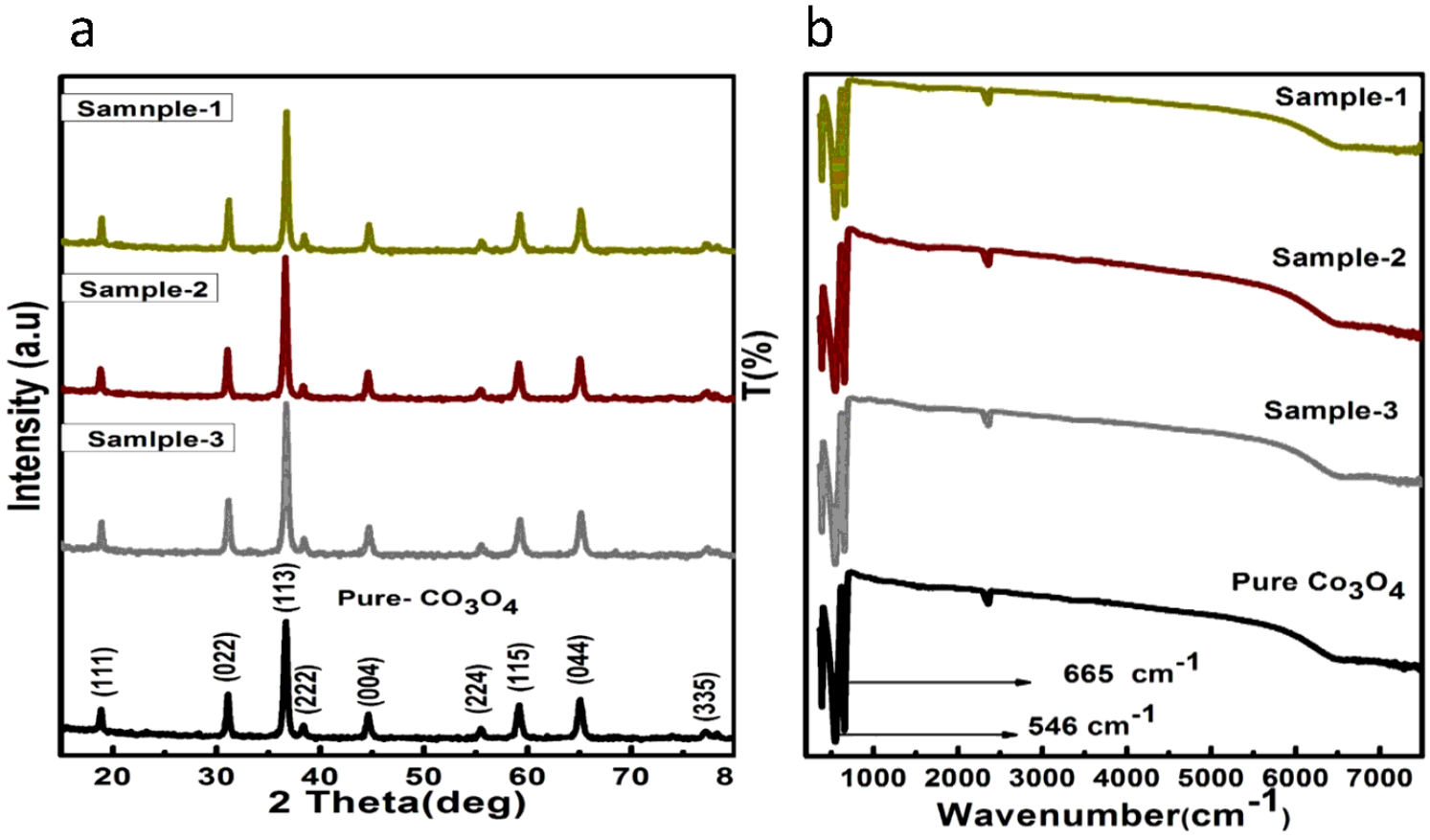

Figure 3

a. XRD diffraction patterns for pure Co3O4, sample 1, sample 2 and sample 3, b. The corresponding FTIR spectra

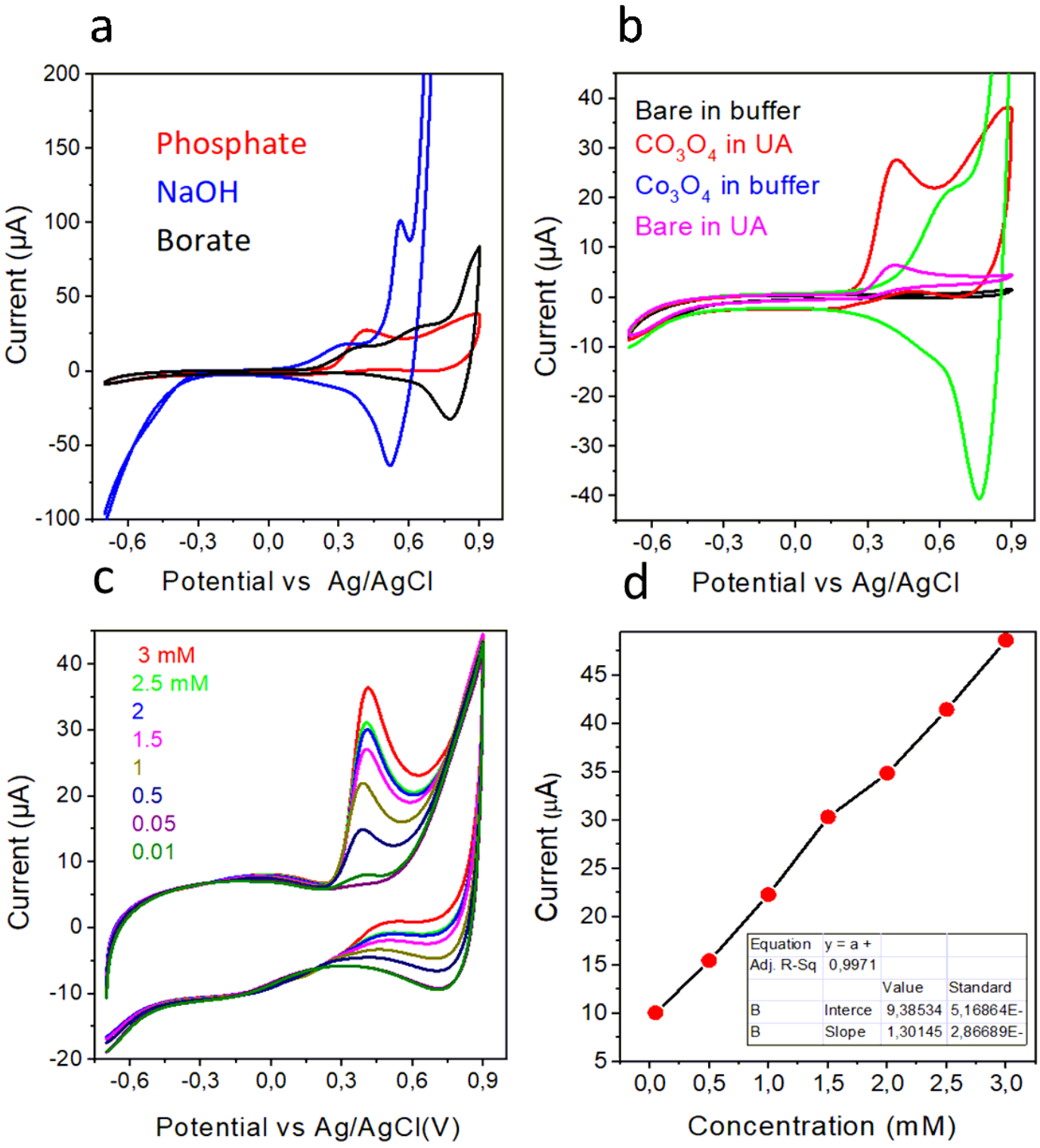

Figure 4

a. CV curves of sample 3 in 0.1M BRB buffer, 0.1M NaOH, 0.1M phosphate buffer, at 50 mV/s b. CV curves of sample 3 (red) in uric acid and (pink) in buffer and bare glassy carbon electrode (black) in buffer, (green) in uric acid at 50 mV/s, c. CV curves in different concentrations of uric acid phosphate buffer solution pH 7.3 at at 50 mV/s, d. linear fitting of oxidation peak current versus various concentration of uric acid

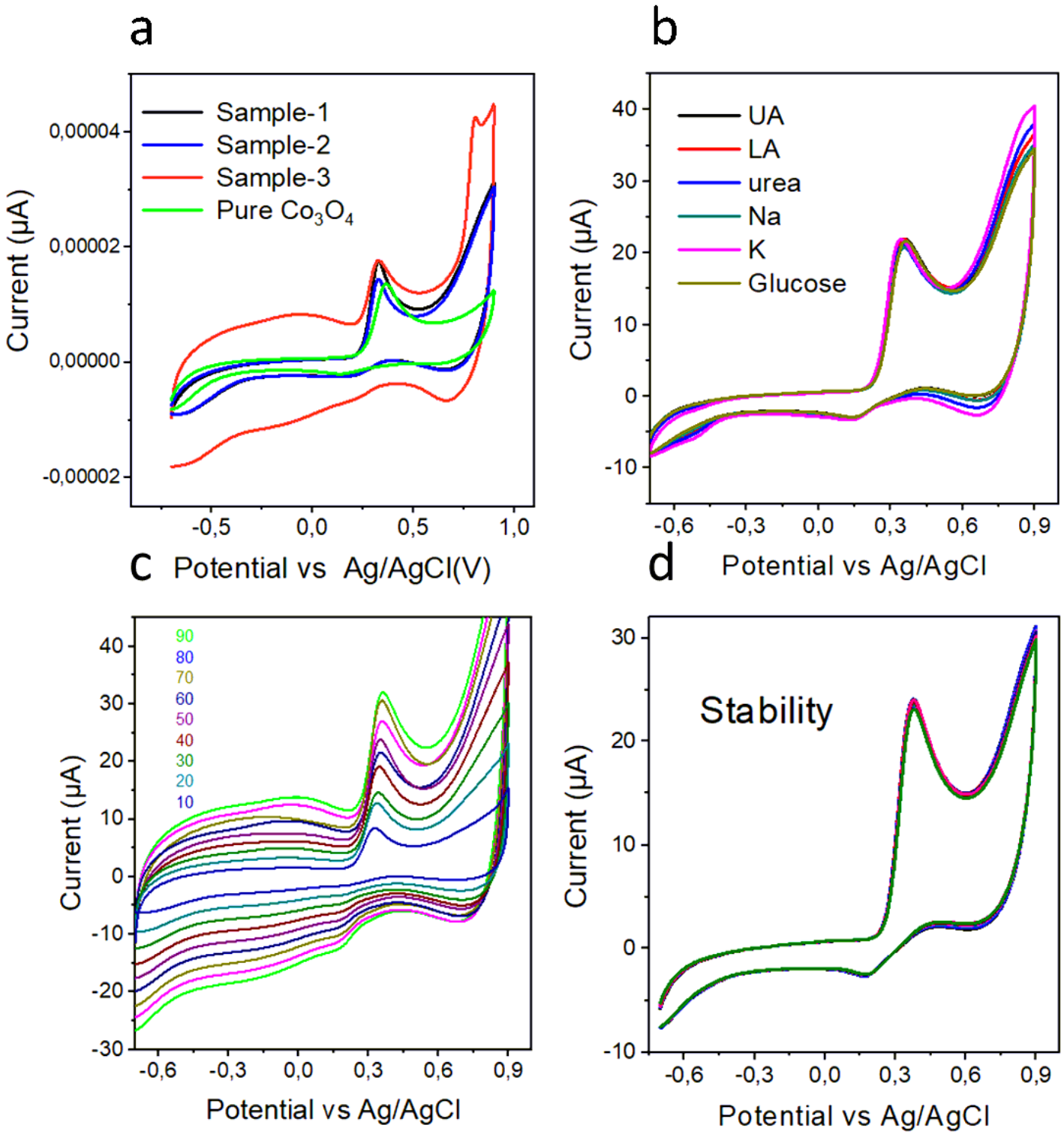

Figure 5

a. CV curves of pure Co3O4, sample 1, sample 2 and sample 3 in 0.1mM uric acid at 50 mV/s, b. CV curves of sample 3 in 0.1 mM uric acid and different interfering species at 50 mV/s, c. scan rate study of sample 3 in 0.1mM uric acid, d. CV curve for the monitoring of stability of sample 3 in 0.1mM uric acid at 50 mV/s.